Possibility of non-Fickian mixing at concentration interface between stratified suspensions

Masahiro Mori[†], Tsubasa Tai[‡], Kosuke Nishimura[†],
Shusaku Harada[†*] and Yasufumi Yamamoto[‡]

[†] Division of Sustainable Resources Engineering, Faculty of Engineering, Hokkaido University,
N13-W8, Sapporo, Hokkaido, 060-8628, Japan
[‡] Department of Mechanical Engineering, Kansai University,
3-35, Yamate-cho 3-chome, Suita, Osaka, 564-8680, Japan

* Corresponding author: Shusaku Harada
Phone/Fax: + (81)-11-7066310
E-mail address: harada@eng.hokudai.ac.jp

ABSTRACT

Hypothesis

Relative motion of micro-sized particles suspended in liquid is governed by hydrodynamic effect, in contrast to nano-sized particle suspension in which thermal effect is significant. As a result, the mixing behavior of stratified suspensions with micro-sized particles is totally different from those obeying Fick's diffusion law for nano-sized particles. Such a “non-Fickian” mixing of micro-sized particles is determined not only by the concentration difference but also the physical properties of suspensions.

Experiments

We conducted an experimental study of gravitational settling of stratified suspensions of micro-sized particles with concentration gradients opposed to gravity. We also performed point-force-type numerical simulations under the same conditions as those in the experiment. Particularly, we focused on the relative motion of particles near the concentration interface, which is an apparent interface between the upper and the lower suspensions having different concentrations.

Findings

The experimental and numerical results indicate that, if the number density of particles in suspension is sufficient, the concentration interface seemingly behaves immiscibly and the interface prevents particle mixing. However, a small number of particles cannot maintain the seal of the concentration interface then demonstrates miscible behavior. The mixing mechanism of the suspended particles at the concentration interface is strongly related to the miscible and immiscible characteristics of the interface.

Keywords: particulate suspension, concentration interface, mixing, gravitational settling

Introduction

Gravitational settling of stratified suspensions is widely seen in global-scale natural phenomena, such as sediment transport [1], deposited layer formation [2], and bio-convection [3], among others. In the engineering fields, this phenomenon has long been systematically studied because of the importance of multiphase processes, such as solid-liquid separation [4].

It is well-known that the settling velocity of suspended particles depends on the concentration, which causes complicated settling behaviors [5]. For example, in stratified suspensions with a positive concentration gradient in the direction of gravity, often observed during settling of suspended solids in a liquid-filled container, the particles in the dilute upper suspension settle faster than those in the dense lower suspension. In this case, the interface between the two differently concentrated suspensions (concentration interface) moves upward or downward to satisfy mass conservation of the settling particles. The concentration interface maintains a flat and clear surface, and the concentration profile evolves almost one-dimensionally in such a system. Known as the "self-sharpening effect," this behavior results from the complicated dependency of the mass flux of the settling particles on the concentration [5].

On the contrary, the settling of stratified suspensions having a concentration in opposition to gravity cannot be explained by the difference in the settling velocity of suspensions with different concentrations. Density-driven instability (Rayleigh–Taylor instability) is widely known to occur at the interface between the high-density upper fluid and the low-density lower fluid [6]. In general, Rayleigh–Taylor instability can be seen at immiscible interfaces (e.g., an oil-water interface), miscible interfaces (e.g., a saltwater-freshwater interface), and at concentration interfaces in particulate suspensions [7-14]. In a suspension, the particles settle hundreds of times faster than the terminal velocity of an isolated particle due to the convective flow caused by the instability at the concentration interface.

Such complicated concentration interface behavior affects the relative motion of the suspended particles. Herein we consider the mixing of particles at the concentration interface between two stratified suspensions with different concentrations. When the particle size is adequately small, such as for nano-

sized particles, the gravitational force is minor and the thermal effect (Brownian force) is significant. In this case, particles mix across the concentration interface according to Fick's law of diffusion.

However, the mixing of stratified suspensions with micro-sized particles exhibits entirely different dynamics. If the concentration gradient is positive in the gravitational direction, mixing occurs due to hydrodynamic diffusion (diffusion caused by hydrodynamic interaction of the suspended particles) [15], in addition to mass transport of particles across the concentration interface. However, if the concentration gradient is negative, the particle mixing behaviors are influenced by a dynamic property of the concentration interface (miscibility), as well as the above-mentioned density-driven instability. The concentration interfaces of micro-sized particle suspensions occasionally behave immiscibly due to the flow induced by individual particle motion [10,12]. If the number density of the particles in the suspensions are adequately large, the concentration interface prevents the intrusion of fluid flow and particles from the outside. Previous studies have quantitatively demonstrated that the macroscopic nature of a concentration interface formed by micro-sized particles can be interpreted as a "miscible interface without diffusion" or an "immiscible interface without interfacial tension" [11]. Therefore the concentration interface miscibility is also important when considering micro-sized particle mixing.

In order to clarify the role of the concentration interface in particle mixing, experimental and numerical analyses of the gravitational settling of stratified suspensions with different concentrations were undertaken. We examined the particle and fluid flow motion near the concentration interface between two suspensions with negative concentration gradients. Based on the experimental and numerical results, we discuss the possibility of non-Fickian mixing of micro-sized particles under gravitational conditions.

Experimental method

Figure 1 shows the schematic diagram of the experimental apparatus. The test cell is a rectangular acrylic vessel with height L = 12 mm, width T = 6 mm, and thickness D = 3 mm. The cell has a horizontal slit on its back side. A thin blade was inserted into the slit to partition the cell into the upper

and lower suspension sections. The blade was a stainless-steel plate with a 0.5 mm thickness. The upper and lower suspensions consisted of acrylic particles and silicone oil. We use mono-dispersion acrylic particles (Chemisnow MX-3000, Soken-Chemical and Engineering) with very narrow size distribution. The mass density of each particle was ρ_p = 1190 kg/m^3 and the average diameter d_p = 30 μm. The mass density and viscosity of the silicone oil (Element14 PDMS100-J, Momentive Performance Materials) were ρ_f = 972 kg/m^3 and μ_f = 100 mPa·s, respectively. The suspension was mixed by a magnetic stirrer for tens of minutes to prevent air from intrusion in the liquid.

In order to control the "collectivity" of the suspensions, we modified the particle concentration in each suspension. In the previous study [10], the following dimensionless parameter, which describes the dynamic property of suspension, was defined as the ratio of the length scale of the flow path (cell thickness D) to the average particle distance $d_p/\phi^{1/3}$ (d_p: particle diameter, ϕ: particle volumetric ratio) as

$$C = \frac{D}{d_p}\phi^{1/3}. \tag{1}$$

The dimensionless parameter describes the transition from continuum to particle-like suspension behavior well. The suspended particles behave as individuals relative to fluid for C values below 2.16 (particle-like condition) and they settle down almost with the terminal velocity of an isolated particle (Stokes settling velocity). On the other hand, the suspended particles behave perfectly as a continuum when C is greater than14.4 (fluid-like condition). Under this condition, the settling velocity is much faster than the Stokes settling velocity. For values of C between 2.16 and 14.4, the collective and individual behaviors of the suspended particles coexist (intermediate condition) [10]. In this study, the mixing behaviors of various combinations of suspensions with different collectivities were examined.

The experimental procedure is described as follows: First, the lower part of the experimental cell was filled with the low concentration (low collectivity) suspension until the surface reached the position of the slit. Then, the stainless blade was put into the cell and the high concentration (high

collectivity) suspension was input into the section above it. Subsequently, the blade was removed, and the settling behavior of the suspended particles was recorded by a digital video camera. Especially we focused on the particle behavior near the concentration interface between the upper and lower suspensions. The successive pictures were taken from digital video data for a certain period and the lowermost position of concentration interface at each instant of time was detected by image analysis.

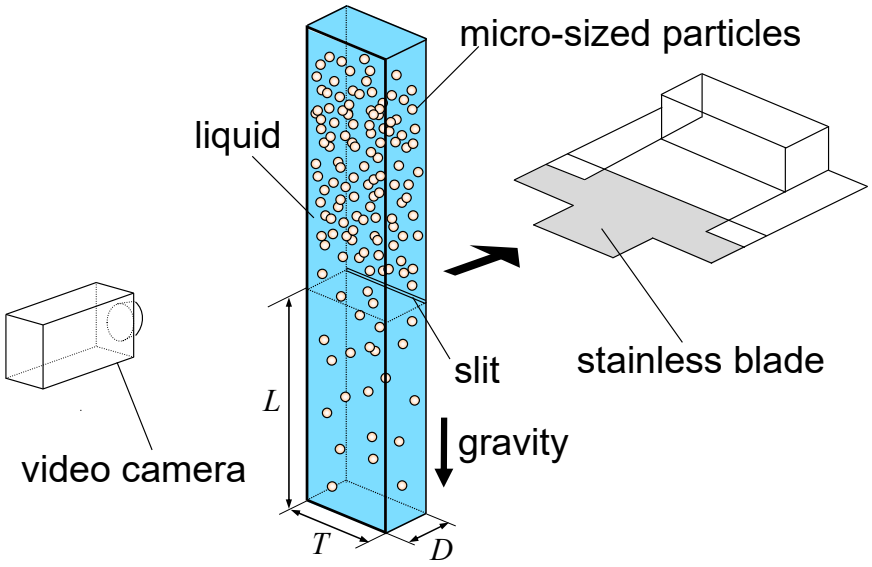

Fig.1 Schematic diagram of the experimental system.

Numerical method

We employed Lagrangian tracking of individual particles with two-way coupling using a point-force model, as in previous studies [12,16]. By assuming that the particle response time was much smaller than the fluid flow time scale, and consequently the Stokes number was much smaller than one, we could neglect the particle inertia. In this case, we considered particle motion resulting only from Stokes drag and gravity, without inertia, as:

$$0 = -3\pi\mu d_p\big(\boldsymbol{v} - \boldsymbol{u}(\boldsymbol{y})\big) + \frac{\pi}{6} d_p^3(\rho_p - \rho_f)\boldsymbol{g}, \tag{2}$$

where $\boldsymbol{v}$ and $\boldsymbol{u}$ are the particle velocity and fluid velocity at particle position $\boldsymbol{y}$, respectively, and $\boldsymbol{g}$ is the acceleration due to gravity. The particle velocity was instantaneously solved using the above

equation with the interpolated fluid velocity at the particle position, and the particle position was subsequently updated by integration. We used the second-order Adams–Bashforth method for integrating particle position.

In simple terms, the relative velocity used to compute the Stokes drag for a single particle falling in a stationary liquid is not the velocity field dragged by the target particle, but the far field. Therefore, the fluid velocity at the particle position should be determined by the velocity field that does not include the effect of the target particle. However, considering only the far field is not suitable for the case in which other particles are present close to the target particle. Thus, we used the velocity averaged over the wide region containing the target particle. Based on verification data of the previous study [12], the averaging region size $5(\Delta d_p)^{1/2}$ (where Δ is the fluid computation cell size) was employed, which reduced the relative error to less than 10%, regardless of particle size and position relative to the computational cell.

We applied the point-force model to the particle and considered the particle to have no volume. The fluid was assumed to be incompressible and its motion described by the continuity equation

$$\nabla \cdot \boldsymbol{u} = 0, \tag{3}$$

and the two-way-coupled Navier-Stokes equation

$$\rho_f \left(\frac{\partial \boldsymbol{u}}{\partial t} + \nabla \cdot \boldsymbol{u}\boldsymbol{u} \right) = -\nabla p + \mu \nabla^2 \boldsymbol{u} + \boldsymbol{f}, \tag{4}$$

where $\boldsymbol{f}$ is the feedback force per unit volume, given by

$$\boldsymbol{f}(\boldsymbol{x}) = \frac{1}{\Delta^3} \sum_{\boldsymbol{y}} 3\pi\mu d_p \big(\boldsymbol{v} - \boldsymbol{u}(\boldsymbol{y})\big) w(\boldsymbol{x} - \boldsymbol{y}), \tag{5}$$

where $\boldsymbol{x}$ is the grid-position. The function w is a nondimensional weighting function, and the trilinear distribution to the eight neighboring points is given by w as outlined in [16]. The fluid flow field was obtained by solving Eqs. (3) and (4) with Eq. (5). Equations (3) and (4) were spatially discretized by

the second-order central finite-difference method using a staggered-grid system. The second-order Adams–Bashforth method was applied to advance the advection term in time, while the second-order Crank–Nicolson scheme was used for the viscous term. Pressure was linked to Eq. (3) using the simplified marker and cell algorithm, and the Poisson equation for pressure correction was solved using the biconjugate gradient stabilized method [17].

The number of grid points for D, T, and L were set to 8, 16, and 48, respectively. The resolution was validated by quantitatively comparing results with the experimental one as shown later. The time step was set to 1×10^{-4} s, except for the case with the greatest number of particles as shown in Fig. 2, which had 0.5×10^{-4} s. The number of particles treated under that maximum condition was 114591, and the computational time was about 26 days. As initial conditions, both the particle and fluid velocities were set to zero and the particle positions were decided using random numbers.

Results and discussion

Settling behavior of suspension

In order to examine the mixing behavior of stratified suspensions, we conducted settling experiments on suspensions with various collectivity conditions. Figures 2, 3 and 4 depict experimental observations of suspension settling in rectangular channels along with the numerical results obtained from the particle tracking simulation performed using the corresponding experimental conditions. As mentioned above, the suspension consisted of the same particles (mono-dispersed acrylic particles) and silicone oil, while the collectivity of the suspension was controlled by changing the particle concentration. Figure 2 illustrates the results for the condition in which the upper concentration (volumetric ratio) was $\phi_1 = 0.01$ ($C = 21.5$), while the lower concentration was $\phi_2 = 0.005$ ($C = 17.1$), and thus both suspensions were in fluid-like conditions with high collectivities (F-F condition) [10]. The conditions of Fig.3 were an upper concentration $\phi_1 = 0.005$ ($C = 17.1$) and a lower concentration $\phi_2 = 0.002$ ($C = 12.6$). In this case, the upper suspension was in a fluid-like condition while the lower was in an intermediate condition (F-I condition). The conditions reflected

in Fig.4 were an upper concentration $\phi_1 = 0.002$ ($C = 12.6$) and lower concentration $\phi_2 = 0.001$ ($C = 10.1$), and thus both suspensions were in intermediate conditions (I-I condition).

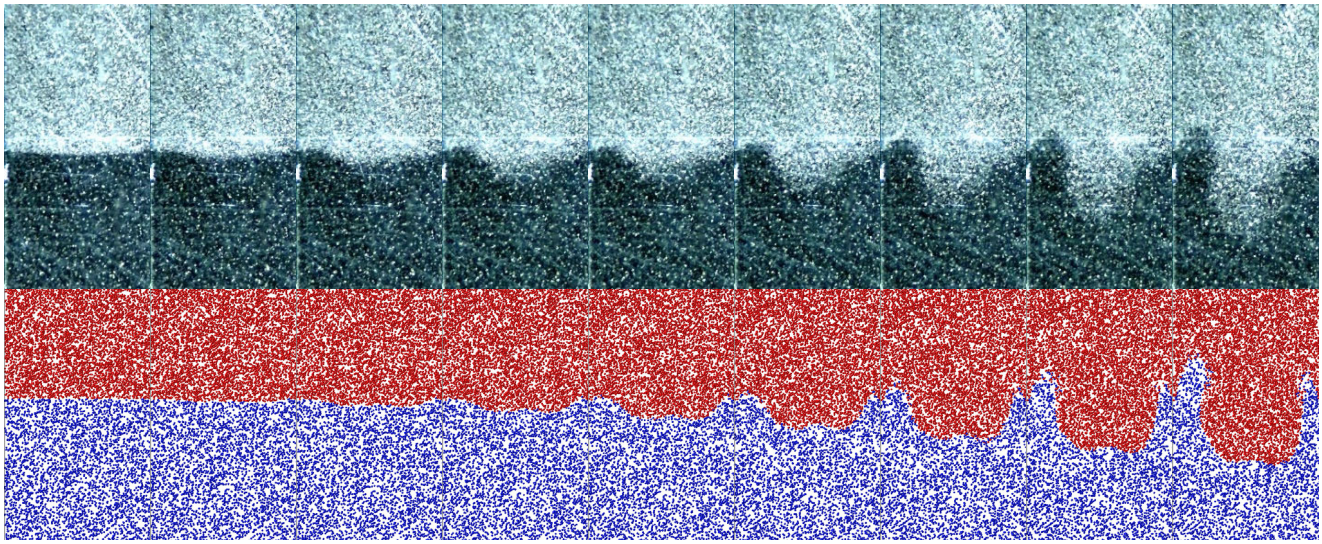

Fig.2 Settling behavior of particulate suspensions near the concentration interface for $\phi_1 = 0.01$ and $\phi_2 = 0.005$ (upper: experimental results, lower: numerical results).

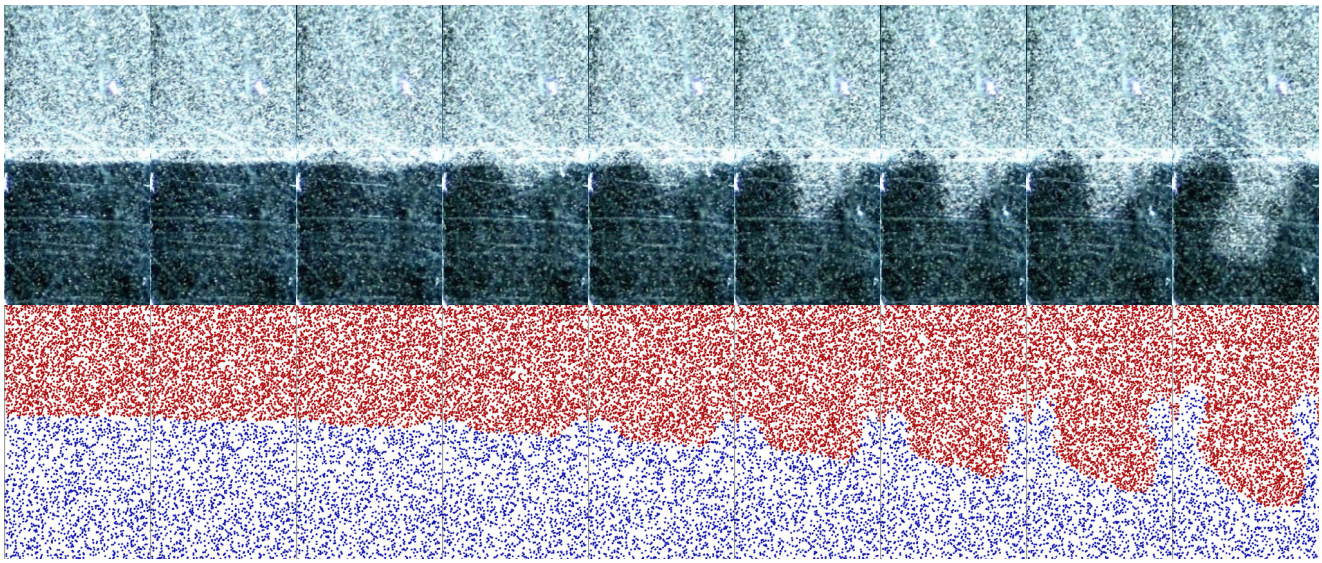

Fig.3 Settling behavior of particulate suspensions near concentration interface for $\phi_1 = 0.005$ and $\phi_2 = 0.002$ (upper: experimental results, lower: numerical results).

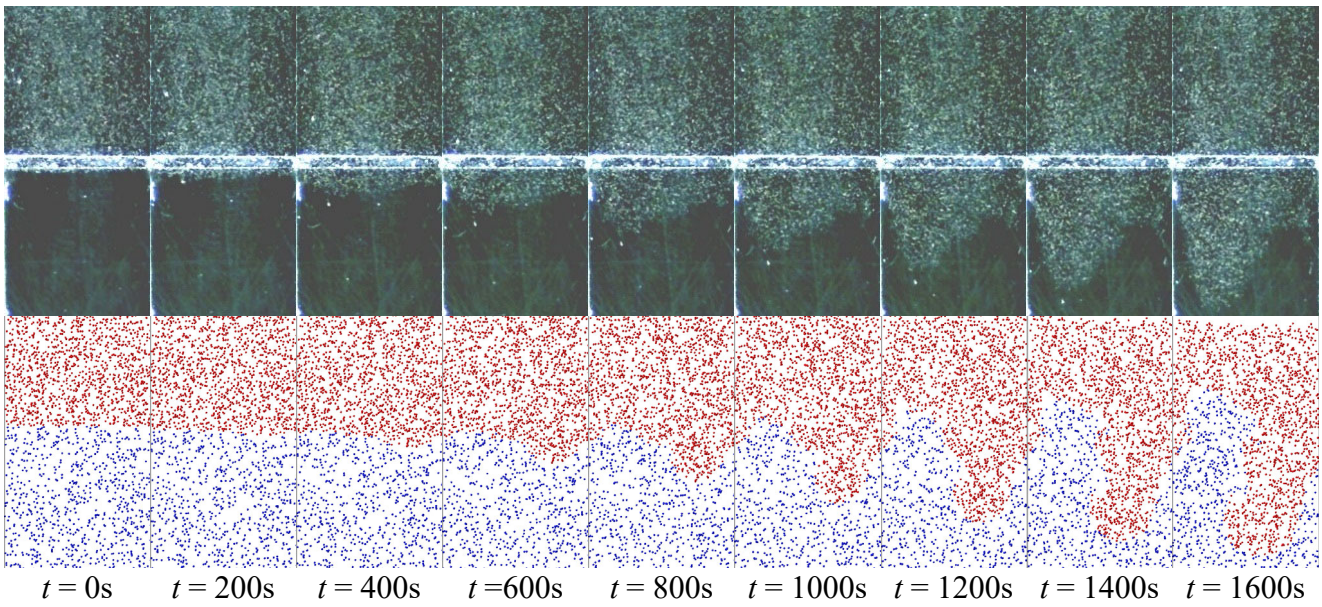

Fig.4 Settling behavior of particulate suspensions near concentration interface for $\phi_1 = 0.002$ and $\phi_2 = 0.001$ (upper: experimental results, lower: numerical results).

The numerical results in Figs.2–4 show cross-sectional views, symbolizing only the central region particles located at 0.1*D* thickness in the depth direction, whereas the experimental results show side views of the experimental cell. The width of each picture corresponds to the width of the experimental cell *T*. As can be seen in these figures, a finger-like blob of the upper suspended particles settles down near the center of the experimental cell. This feature is especially similar to Rayleigh–Taylor instability at the interface between two immiscible fluids or concentration interface between a particulate suspension and a pure fluid in a rectangular cell [11,18]. According to the previous study of Rayleigh–Taylor instability of a suspension-fluid interface, the upper suspended particles invade into the lower pure fluid collectively as a mass with a half-length of the cell width [11].

Figures 2 through 4 show that the simulated behavior of the suspended particles obtained from the numerical analysis is similar to the experimental observations under the corresponding conditions. The numerical and experimental results indicate that the suspension settling behavior depends on the collectivity of each suspension. When the collectivity of the upper suspension is large (as in Figs.2 and 3), a clear concentration interface is formed, and a nearly symmetric suspension blob settles down

in the central part of the channel. In contrast, when neither the upper and lower suspensions are large (Fig.4), the concentration interface become unclear, and an asymmetric finger-like blob is formed.

In order to quantitatively verify the agreement of the numerical and experimental results, the settling velocity of the particles at concentration interface was estimated. Figure 5 shows the temporal change in the vertical position of the concentration interface (the tip of the finger) obtained from both experimental and numerical results. The finger initially grows exponentially with time, and subsequently begins to grow linearly. As demonstrated by the figures, the numerical results agree well with the experimental results with respect to finger growth. More quantitatively, we estimated the settling velocity from a linear fit of the fingertip positions, wherein the slope was defined as the

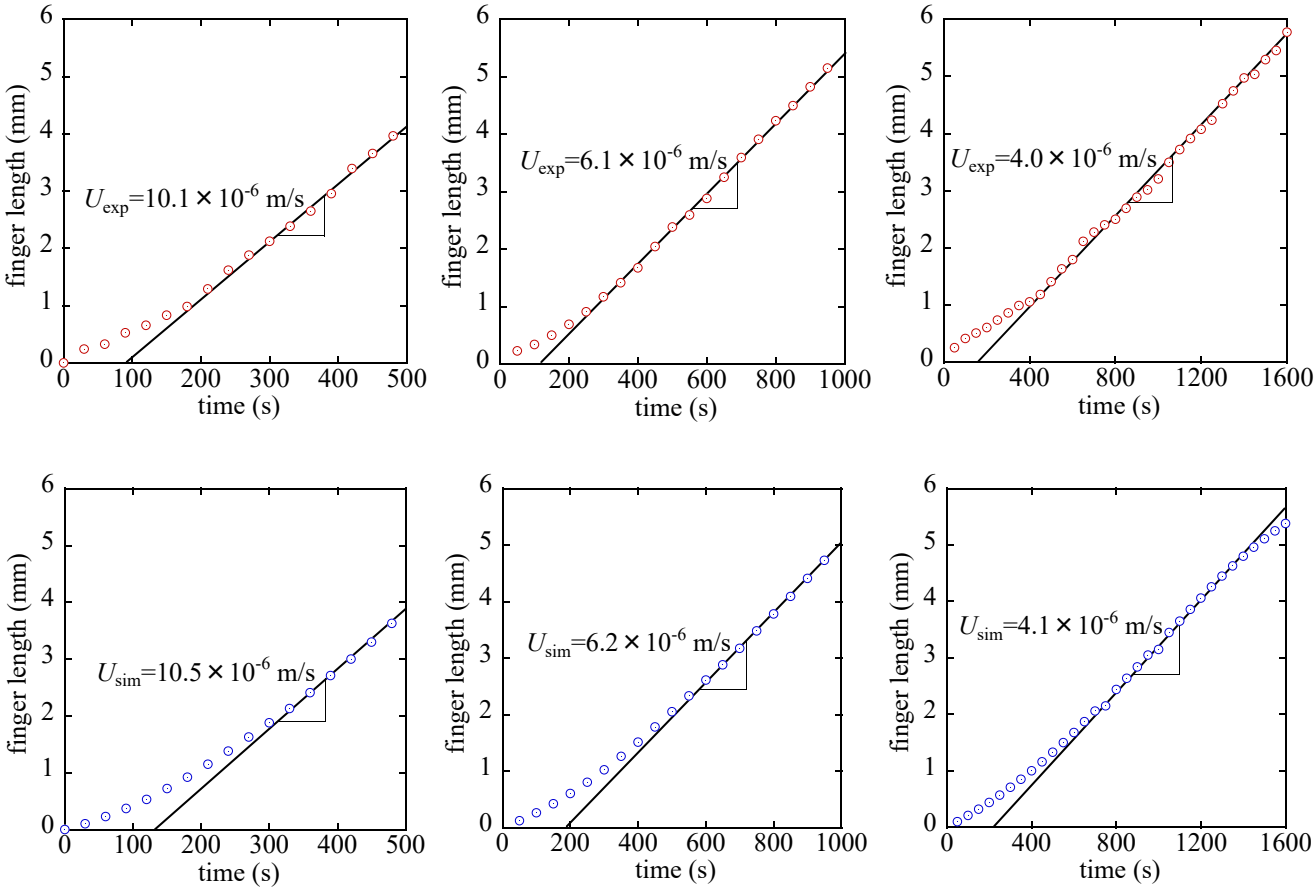

(a) $\phi_1 = 0.01$, $\phi_2 = 0.005$ (b) $\phi_1 = 0.005$, $\phi_2 = 0.002$ (c) $\phi_1 = 0.002$, $\phi_2 = 0.001$

Fig.5 Temporal change in vertical length of fingers (upper: experimental results, lower: numerical results).

settling velocity of the upper suspension. The obtained settling velocities were U_{exp}=10.1×10^{-6} m/s and U_{sim}=10.5×10^{-6} m/s (for fluid-like vs. fluid-like), U_{exp} = 6.1×10^{-6} m/s and U_{sim}=6.2×10^{-6} m/s (for fluid-like vs. intermediate), and U_{exp}=3.9×10^{-6} m/s and U_{sim} = 4.1 × 10^{-6} m/s (for intermediate vs. intermediate), respectively.

Figure 6 shows the settling velocity for each condition, normalized by the Stokes settling velocity, $U_{St} = (\rho_p - \rho_f)\, d_p^2 g/(18\mu)$. As seen in Fig.6, the numerical and experimental results agree for similar conditions. This quantitative agreement of the settling velocity values reveals that the numerical analysis can sufficiently reproduce the actual suspension settling behaviors by the present resolution setting. It is also clear from Fig.6 that the suspension settling velocity values are several times larger than the Stokes settling velocity. These results indicate that collective behavior of suspension increases the settling velocity above that of an isolated particle. Further quantitative discussion of the settling velocity is presented later.

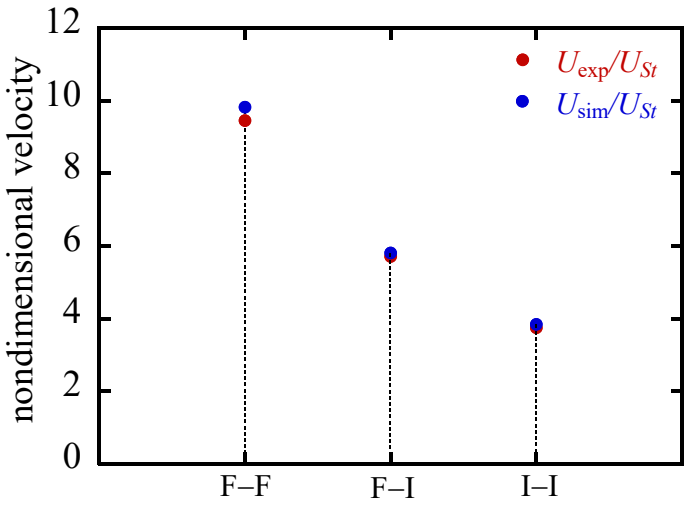

Fig.6 Settling velocity of suspended particles at the tip of the concentration interface, normalized by the Stokes settling velocity for the F–F (fluid-like vs. fluid-like), F–I (fluid-like vs. intermediate), and I–I (intermediate vs. intermediate) conditions.

Sealing of fluid flow at concentration interface

Figure 7 shows the streamlines of the fluid velocity relative to finger tip's vertical settling velocity obtained from the numerical analysis under high and low collectivity conditions, corresponding

Figs.2 through 4. In cases in which the upper suspension has a high collectivity (Figs.7(a) and (b)), the lower suspension rises on both sides of the cell, avoiding the centered settling finger-like bulge of the upper suspension. As seen in Figs.7(a) and (b), there is no streamline crossing the concentration interface. In other words, immiscible behavior is observed at the concentration interface when the collectivity of the upper suspension is large. Consequently, no mixing occurs between the upper and lower particles. Contrastingly, in Fig.7 (c), the lower suspension rises on one side of the flow path and streamlines cross the concentration interface. These results imply that when the upper and lower suspension collectivities are small, the concentration interface behaves as a miscible interface, and may cause particle mixing.

The consistency between the experimental and numerical results, ignoring the particle volume, suggests that the shielding property of the concentration interface is influenced by the flow caused by the particle as a point force (Stokeslet). As suggested in the previous studies [19-21], if the Stokeslet exists sufficiently at the concentration interface (in the case of large collectivity), the flow caused by individual particle motion prevents flow intrusion from the outside. Therefore, the concentration interface is shielded, and particle mixing does not occur. However, if the Stokeslet number density is insufficient (in the case of small collectivity), the concentration interface loses its shielding ability, and consequently particle mixing may occur. Based on the above results, it is clear that the Stokeslet number density of the upper suspension determines the shielding property of the concentration interface, and greatly affects the upper and lower particle mixing. These features are particular to suspensions with micro-sized particles. As mentioned in the introduction, if the suspension consists of nano-sized particles, Fickian-type diffusion is dominant at the concentration interface between suspensions of different concentrations, and thermal effect causes particle mixing across the interface. On the other hand, the mixing of stratified suspensions of micro-sized particles is greatly influenced

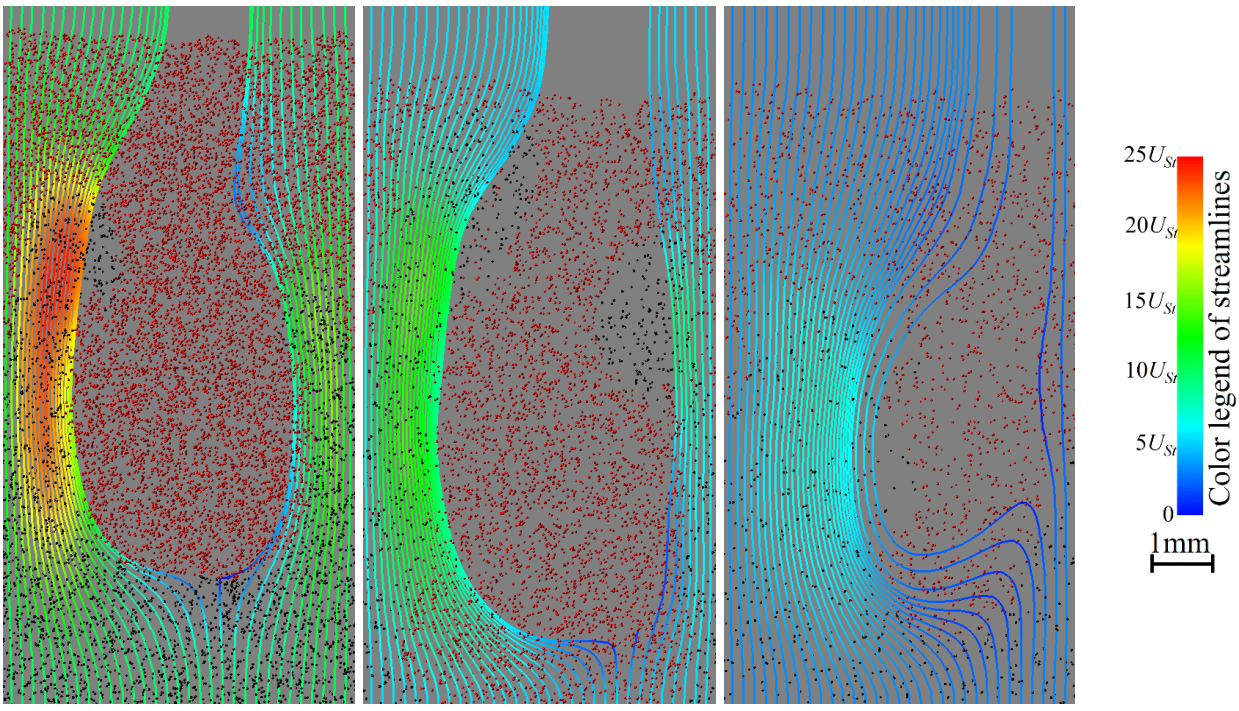

(a) F-F condition (b) F-I condition (c) I-I condition

Fig.7 Streamlines of fluid velocity relative to finger tip's settling velocity obtained from numerical results.

by the dynamic properties of the suspensions, namely, the collectivity of each suspension and the shielding of the concentration interface. Consequently, the mixing behaviors of micro-sized particles in liquid must be considered from non-Fickian point of view.

Quantitative discussion of settling velocity

In order to examine the settling velocity of stratified suspensions more quantitatively, we performed the experiment and numerical simulation under various particle and fluid conditions. Figure 8 shows the settling velocity at the concentration interface of various suspensions, normalized by the Stokes settling velocity. The suspended particles were mono-dispersed acrylic particles with various diameters. The fluid was silicone oil with a viscosity μ = 100 mPa·s, except that μ = 10 mPa·s in the case of the smallest settling velocity (particle diameter d_p=30μm, concentration difference $\phi_1-\phi_2$=0.0005).

It can be seen from Fig.8 that the nondimensional settling velocity is larger when a larger concentration difference exists between the upper and lower suspensions. This is because a large

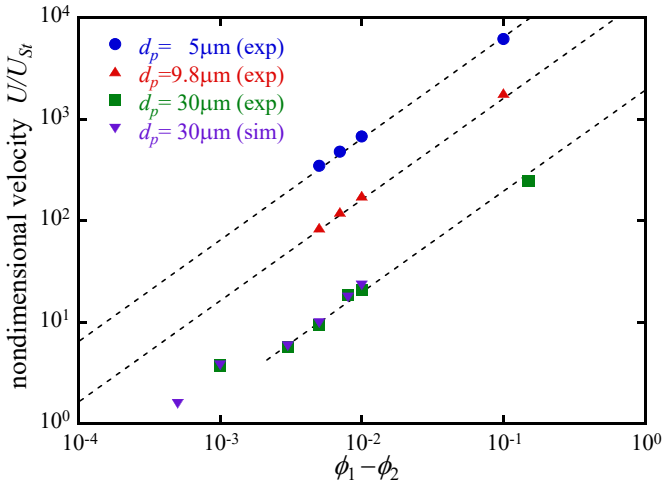

Fig.8 Nondimensional velocity of suspended particles at the tip of concentration interface for various suspensions.

concentration difference enhances the growth rate of the Rayleigh–Taylor instability and the finger-like blob settles very fast. As also demonstrated in Fig.8, the nondimensional velocity is larger in the suspensions with small particles. A detailed discussion of the size dependency will be provided later.

Figure 8 also indicates that the nondimensional velocity is a function of the concentration difference, $\phi_1 - \phi_2$, for each particle size, except for the small concentration difference of large particles (d_p = 30μm). In most of these conditions, the upper suspension corresponds to high collectivity, C >14.4 (fluid-like condition), and behaves as a continuum. Therefore, the suspension settles as an immiscible blob into the lower suspension.

Here, we consider the settling velocity of a finger-like suspension blob into the lower suspension. As described in the previous study [11], the settling velocity of a disk-shaped suspension blob with diameter λ and thickness D can be determined based on balancing the gravitational and buoyancy force ($\sim\Delta\rho\lambda^2 Dg$) and the drag force ($\sim\mu\lambda U$), where $\Delta\rho = \rho_1 - \rho_2$ is the difference between the density of the upper suspension $\rho_1 = \phi_1\rho_p + (1-\phi_1)\rho_f$ and that of the lower suspension $\rho_2 = \phi_2\rho_p + (1-\phi_2)\rho_f$. From these relations, the settling velocity can be written as:

$$U \sim \frac{(\phi_1 - \phi_2)(\rho_p - \rho_f) g \lambda D}{\mu}. \quad (6)$$

In the above equation, the diameter of a disk, λ, corresponds to the horizontal finger length, and should be proportional to the cell width, T, in the rectangular channel. Therefore, the settling velocity can be written as:

$$U \sim \frac{(\phi_1 - \phi_2)(\rho_p - \rho_f) g T D}{\mu} \sim \frac{T}{D}\left(\frac{d_p}{D}\right)^{-2}(\phi_1 - \phi_2)\frac{(\rho_p - \rho_f) g d_p^2}{\mu}. \quad (7)$$

The last segment of the above equation has the same form as the Stokes settling velocity $U_{St} = (\rho_p - \rho_f)\, d_p^2 g/(18\mu)$. Consequently, the nondimensional velocity is obtained in the following form:

$$\frac{U}{U_{St}} = K\frac{T}{D}\left(\frac{d_p}{D}\right)^{-2}(\phi_1 - \phi_2), \quad (8)$$

where K is constant. Based on the previous discussion, if the concentration interface is immiscible and the finger-like blob behaves as a continuum, the settling velocity of the upper suspension into the lower suspension will be determined by the concentration difference $\phi_1 - \phi_2$, the ratio of particle diameter to cell thickness d_p/D, and the cross-sectional aspect ratio of the cell T/D.

Figure 9 plots of the settling velocity of suspensions at the concentration interface along the horizontal axis of $(d_p/D)^{-2}(\phi_1 - \phi_2)$. As can be seen from Fig.9, the experimental and numerical results demonstrate a linear relationship with the horizontal axis for almost all conditions. However, for small horizontal axis values, the settling velocity deviates from the relation given by Eq. (8).

As discussed above, Eq. (8) is derived under the assumption that the upper suspension settles as a continuum, immiscible to the lower suspension. Therefore, if the settling velocity satisfies the relation given in Eq. (8), the concentration interface is immiscible, and mixing of the upper and lower suspensions does not occur. Conversely, under conditions in which the settling velocity does not obey Eq. (8), particle mixing may occur due to the insufficiently sealed concentration interface.

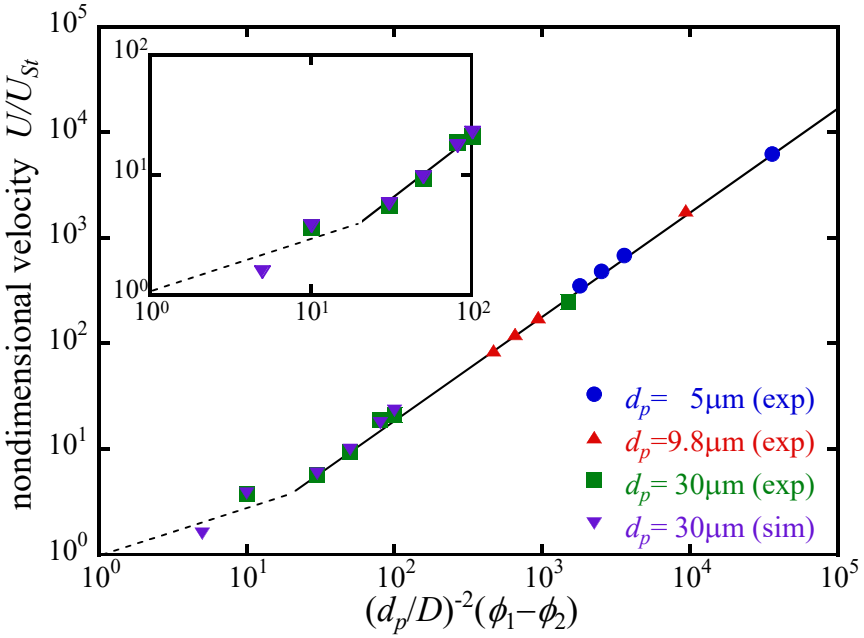

Fig.9 Scaling of nondimensional velocity of suspended particles at the tip of the concentration interface for various suspensions.

The deviation from Eq. (8) at small horizontal axis values in Fig.8 can be explained using another approach. The horizontal axis equation in Fig.8 can be rewritten as:

$$\left(\frac{d_p}{D}\right)^{-2}(\phi_1-\phi_2)=\left(\frac{D}{d_p}{\phi_1}^{1/2}\right)^2-\left(\frac{D}{d_p}{\phi_2}^{1/2}\right)^2. \tag{9}$$

Therefore, the horizontal axis in Fig.8 can be roughly expressed as the difference of the squares of collectivity C ($=D\phi^{1/3}/d_p$) of the upper and the lower suspensions, except for insensitive function $\phi^{1/6}$. Consequently, if this value is larger, collectivity condition of the upper suspension is larger than that of the lower suspension. On the other hand, as the horizontal axis decreases, the difference in collectivity approaches zero, and the upper and the lower particles behave as one suspension regardless of their collectivity. In such a case, the settling velocity would approach the Stokes settling velocity U_{St} and the mixing would occur due to the hydrodynamic diffusion of suspended particles [15,22].

Further discussion of the collectivity definition is given in the previous study [12]. If we express Eq. (9) using the modified collectivity $C_{\mathrm{mod}}=C\phi^{1/6}$, proposed in [12], it can be written as:

$$\left(\frac{d_p}{D}\right)^{-2}(\phi_1-\phi_2)=C_{\mathrm{mod}\,1}^2-C_{\mathrm{mod}\,2}^2=(C_{\mathrm{mod}\,1}+C_{\mathrm{mod}\,2})(C_{\mathrm{mod}\,1}-C_{\mathrm{mod}\,2}). \tag{10}$$

According to Eq. (10), the settling velocity of stratified suspensions can be simply determined as the product of the average value and the difference of the upper and the lower suspension collectivities. The above results indicate that the settling behavior of the concentration interface between two stratified suspensions with different concentrations can be predicted quantitatively. Furthermore, the mixing characteristics of particles across the concentration interface can also be predicted from the suspension conditions.

Conclusions

Gravitational settling of stratified suspensions has long been systematically studied because of the importance of multiphase processes in many fields [1-4]. We experimentally and numerically investigated gravitational settling of stratified suspensions of micro-sized particles in which the concentration gradient opposed the gravity. In such a system, it is known that the density-driven instability (Rayleigh–Taylor instability) occurs at the concentration interface, which is the ambiguous interface between the two suspensions, and the suspended particles settle as a finger-like blob much faster than an isolated particle [7,8]. The concentration interface behaves in a miscible or immiscible manner depending on the “collectivity” of the upper suspension [10-12].

The above-mentioned collective nature of suspensions with micro-sized particles bring about entirely different mixing dynamics at the concentration interface, from that of nano-particles according to Fick’s law of diffusion. In order to examine the possibility of “non-Fickian” mixing of micro-sized particles in liquid, we investigated the mixing of particles between two stratified suspensions with different concentrations. In this study, the following new findings were obtained.

- If the concentration of the upper suspension is sufficiently large, the concentration interface

seals out the fluid flow intrusion and particles from the outside. Consequently, particle mixing does not occur.

- In such a case, the particle settling velocity is proportional to the concentration difference and the square of the ratio of particle diameter to the flow cell thickness.
- If the concentration difference between the upper and lower suspension is adequately small, the upper and lower suspensions settles as one body, and the settling velocity approaches the terminal velocity of an isolated particle.

Thus, we showed new conceptual advances of mixing of micro-sized particles in liquid, i.e., the miscibility of concentration interface of stratified suspensions, which is determined by "collectivity" of suspension, affects the mixing of particles across the interface. In contrast to nano-sized particle behavior, the mixing of micro-sized particles demonstrates complicated non-Fickian features. The mixing behavior depends not only on the properties of the fluid and the particle but also on the dynamic property (miscibility) of the concentration interface between the two suspensions.

In future, we plan to examine mixing behaviors of suspended particles at concentration interface in more quantitative way and establish a physical model describing such a non-Fickian mixing of micro-sized particles.

Acknowledgment

This study was supported by JSPS KAKENHI Grant Number 26420095 and 19H02058.

References

[1] Hoyal, D.C.J.D., Bursik, M.I., Atkinson, J.F., 1999. Settling-driven convection: a mechanism of sedimentation from stratified fluids. J. Geophys. Res. 104, 7953–7966.
[2] Carey, S., 1997. Influence of convective sedimentation on the formation of widespread tephra fall layers in the deep sea. Geology 25, 839–842.
[3] Pedley, T.J., Kessler, J.O., 1992. Hydrodynamic phenomena in suspensions of swimming microorganisms. Annu. Rev. Fluid Mech. 24, 313–358.
[4] Davis, R. H. and Acrivos, A., 1985. Sedimentation of noncolloidal particles at low Reynolds numbers. Annu. Rev. Fluid Mech. 17, 91–118.
[5] Kynch, G.J., 1952. A theory of sedimentation. Trans. Faraday Soc. 48, 166–176.

[6] Chandrasekhar, S. 1981. Hydrodynamic and Hydromagnetic Stability, Dover Publications, New York.
[7] Voltz, C., Pesch, W., Rehberg, I., 2001. Rayleigh–Taylor instability in a sedimenting suspension. Phys. Rev. E 65, 011404-1–011404-7.
[8] Blanchette, F., Bush, J.W.M., 2005. Particle concentration evolution and sedimentation-induced instabilities in a stably stratified environment. Phys. Fluids 17, 073302-1–073302-11.
[9] Burns, P., Meiburg, E., 2012. Sediment-laden fresh water above salt water: linear stability analysis. J. Fluid Mech. 691, 279–314.
[10] Harada, S., Mitsui, T. and Sato, K., 2012. Particle-like and fluid-like settling of a stratified suspension. Eur. Phys. J. E, 35, 1–6.
[11] Harada, S., Kondo, M., Watanabe, K., Shiotani, T. and Sato, K., 2013. Collective settling of fine particles in a narrow channel with arbitrary cross-section. Chem. Eng. Sci., 93, 307–312.
[12] Yamamoto, Y., Hisataka, F. and Harada, S., 2015. Numerical simulation of concentration interface in stratified suspension: continuum-particle transition. Int. J. Multiphase Flow, 73, 71–79.
[13] Chou, Y.-J., Shao, Y.-C., 2016. Numerical study of particle-induced Rayleigh-Taylor instability: Effects of particle settling and entrainment. Phys. Fluids, 28, 043302.
[14] Shao, Y.-C., Hung, C.-Y., Chou, Y.-J., 2017. Numerical study of convective sedimentation through a sharp density interface. J. Fluid Mech., 824, 513–549.
[15] Guazzelli, E., Hinch, J., 2011. Fluctuation and instability in sedimentation. Ann. Rev. Fluid Mech. 43, 97–116.
[16] Bosse, T., Kleiser, L., Härtel, C., Meiburg, E., 2005. Numerical simulation of finite Reynolds number suspension drops settling under gravity. Phys. Fluids, 17, 037101.
[17] Ferziger, J. H., Perić , M., Computational Methods for Fluid Dynamics, Springer-Verlag (1996).
[18] Kurose, Y., Ishizawa, K., Soriano, M. R. and Harada, S., 2019. Scale-independent model of gravitational dispersion of particulate suspension in fractal channel. Chem. Eng. Sci., 199, 231–239.
[19] Nitche, J. M., Batchelor, G. K., 1997. Break-up of a falling drop containing dispersed particles. J. Fluid Mech., 340, 161–175.
[20] Machu, G., Meile, W., Nitche, L.C., Schaflinger, U., 2001. Coalescence, torus formation and breakup of sedimenting drops: experiments and computer simulations. J. Fluid Mech., 447, 299–336.
[21] Metzger, B., Nicolas, M., Guazzelli, E., 2007. Falling clouds of particles in viscous fluids. J. Fluid Mech., 580, 283–301.
[22] Davis, R. H., 1996. Hydrodynamic diffusion of suspended particles: a symposium. J. Fluid Mech., 310 325–335.